Heliyon 10 (2024) e32337

Contents lists available at ScienceDirect

Heliyon

journal homepage: www.cell.com/heliyon

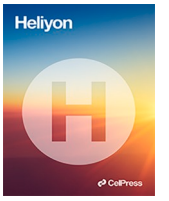

Research article

An anoikis-related gene signature predicts prognosis, drug sensitivity, and immune microenvironment in cholangiocarcinoma

Guochao Liu [a,1], Yujian He [b,1], Zhaoqiang Yin [a,*], Zhijie Feng [b,**]

[a] Department of Minimally Invasive and Biliary Surgery, The Second Hospital of Hebei Medical University, Shijiazhuang, China
[b] Department of Gastroenterology, The Second Hospital of Hebei Medical University, Hebei Key Laboratory of Gastroenterology, Hebei Institute of Gastroenterology, Shijiazhuang, China

ARTICLE INFO

Keywords:
Cholangiocarcinoma
Anoikis-related genes
Prognostic signature
Prognosis
Immune microenvironment

ABSTRACT

Background: Cholangiocarcinoma is a malignant invasive biliary tract carcinoma with a poor prognosis. Anoikis-related genes are prognostic features of a variety of cancers. However, the value of prognostication and therapeutic effect of anoikis-related genes in cholangiocarcinoma have not been reported. The aim of this research was developing an ARGs signature associated with cholangiocarcinoma patients.

Methods: We introduced transcriptome data to discover genes that were differentially expressed in cholangiocarcinoma. Subsequently, WGCNA was utilized to screen critical module genes in reference to anoikis. The univariate Cox, Lasso regression and Kaplan-Meier survival were executed to build a prognostic signature. We further performed gene functional enrichment, immune microenvironment and immunotherapy analysis between two risk subgroups. Finally, the pRRophetic algorithm was applied to compare the half inhibitory concentration value of several drugs.

Results: A grand total of 1844 genes with differential expression related to the cholangiocarcinoma patients were identified. Furthermore, we obtained 2678 key module genes related to anoikis. Then, a prognostic signature was developed using the 6 prognostic genes (*FXYD2*, *PCBD1*, *C1RL*, *GMNN*, *LAMA4* and *HACL1*). Independent prognostic analysis showed that risk score and alcohol could function as separate prognostic variables. We found cetain distinction in the immune microenvironment between the two risk subgroups. Moreover, immunotherapy evaluation showed that the anoikis-related gene signature could be applied as a therapy predictor. Finally, Chemotherapeutic drug sensitivity results showed that the low-risk group responded better to bosutinib, gefitinib, gemcitabine, and paclitaxel, while the high-risk group responded better to axitinib, cisplatin, and imatinib.

Conclusion: The prognostic signature comprised of *FXYD2*, *PCBD1*, *C1RL*, *GMNN*, *LAMA4* and *HACL1* based on anoikis-related genes was established, which provided theoretical basis and reference value for the research and treatment of cholangiocarcinoma.

* Corresponding author.
** Corresponding author.
E-mail addresses: yinzhaoqiang1981@hebmu.edu.cn (Z. Yin), 26300056@hebmu.edu.cn (Z. Feng).
[1] These authors have contributed equally to this work and share first authorship.

https://doi.org/10.1016/j.heliyon.2024.e32337
Received 30 November 2023; Received in revised form 31 May 2024; Accepted 2 June 2024
Available online 3 June 2024

1. Introduction

Cholangiocarcinoma (CHOL) is a highly aggressive cancer of the biliary tract, characterized by its malignant and invasive nature and generally poor prognosis [1]. It can be classified based on tumor location, with two primary subtypes: intrahepatic cholangiocarcinoma (iCCA) and extra-hepatic cholangiocarcinoma (eCCA) [2]. ECCA, in turn, can be further categorized into perihilar cholangiocarcinoma (pCCA) and distal cholangiocarcinoma (dCCA) based on its specific location [3]. Its occurrence has grown over the previous thirty years, making it the second most frequent primary liver tumor [4]. Usually starting slowly, the subsequent clinical signs of CHOL are frequently nonspecific, which mostly connected to biliary obstructions resulting from tumors. Most patients receive a standard diagnosis during the intermediate or advanced disease stages or when there are distant metastases present. Although various treatment options are available, CHOL still has a poor prognosis, with a median overall survival (OS) of 12–31 months [5,6]. Therefore, the development of new treatment approaches is desperately needed for CHOL patients with advanced or metastatic disease.

The anoikis process is a form of apoptosis due to the breakage of cell-extracellular or cell-cell matrix attachments that contributes to maintaining tissue homeostasis by taking away misplaced or shed cells [7]. Anoikis is mostly caused by the interplay of two pathways of apoptosis, such as disruption of mitochondria or activation of cell surface death receptors [8]. Anoikis was first seen in epithelial cells and endothelial cells, which is considered a crucial mechanism for invasion and metastasis of cancer [9]. The resistance to anoikis can help isolated cells bypass the death signaling pathway, enabling cells to survive under unfavorable conditions [10]. Studies have reported that anoikis-related genes (ARGs) are prognostic features in glioblastoma, endometrial carcinoma, lung adenocarcinoma, head and neck squamous cell carcinoma, osteosarcoma [11–15]. However, the value of prognostication and therapeutic effect of ARGs in CHOL have not been reported.

Therefore, this study aimed to identify anoikis-related biomarkers in CHOL and established ARGs-related risk signatures to forecast the survival of CHOL patients. The prognostic characteristics in this study provided a theoretical basis for improving prognostic prediction and selection of treatment approaches for CHOL patients.

2. Materials and methods

2.1. Data source

RNA-seq data of E-MTAB-6389 dataset (training set) were collected from EMBL-EBI database, which included 31 normal samples and 75 CHOL samples. GSE107943 (validation set) was obtained from Gene Expression Omnibus (GEO), which included 27 normal samples and 30 CHOL samples. 35 anoikis-related genes (ARGs) were sourced from MsigDB [16].

2.2. Analysis of differential genes

The 'limma' package [17] was utilized to identify the differentially expressed genes (DEGs) between normal group and CHOL group in E-MTAB-6389 dataset. The adj.*P*.value < 0.05 and $|\log_2 FC|>1$ was determined as the threshold. The 'ggplot2' package was employed to generate a volcano plot illustrating the DEGs [18]. A heatmap was created to display the top 20 DEGs, featuring the top 10 down-regulated and top 10 up-regulated genes.

2.3. Weighted gene coexpression network analysis (WGCNA)

Next, the WGCNA [19] was conducted to select the key module genes with anoikis as a clinical trait. Initially, we clustered the samples and subsequently eliminated outliers to ensure the precision of the analysis. We adopted the Euclidean distance as a metric for the calculation and applied a hierarchical clustering approach in which the COMPLETE algorithm was used for the calculation. Subsequently, we constructed a trait heatmap and sample dendrogram, then determined the soft threshold. Gene similarity was calculated based on adjacency, and the phylogenetic tree among genes was generated. Using the dynamic tree cutting algorithm, modules were segmented, setting the minModuleSize at 100. We filtered significant module genes using $|Cor|>0.3$ and $P < 0.05$. Finally, the key module genes were retained by $|GS|>0.2$ and $|MM|>0.5$.

2.4. Functional exploration of intersection genes

The overlapping genes between DEGs and module genes were identified using a Venn diagram. Gene Ontology (GO) and Kyoto Encyclopedia of Genes and Genomes (KEGG) enrichment analysis of intersection genes were conducted via clusterProfiler package [20]. $P < 0.05$ was selected as criteria.

2.5. Risk score-based subgroup analysis of patients with CHOL

The E-MTAB-6389 dataset ($n = 75$) was defined as the training cohort. The univariate Cox regression was performed on the candidate genes by using the 'coxph' function in the R package, and 6 genes associated with prognosis were screened out in E-MTAB-6389 dataset, where $P < 0.05$ was considered statistically significant. The 'glmnet' package was utilized to employ a least absolute

shrinkage and selection operator (LASSO) regression algorithm, aiming to prevent overfitting during analysis [21] and further build the risk signature. The risk score model calculating formula was: $risk\ score = \sum_{i=1}^{n} \beta i * xi$. In this formula, β refers to the regression coefficient and X refers to the expression value of the gene. Using the median value of the risk score acquired from each sample, CHOL patients with survival information were separated into two risk subgroups (high- and low-). The prognostic accuracy of the model was assessed by Kaplan-Meier (K-M) curves and receiver operating characteristic (ROC) curves (1, 3, 5 years). At the same time, the GSE107943 was regarded as an external verification for the risk model. Ulteriorly, we analyzed the correlation between clinicopathological factors (gender, vascular lnvasio, necrosis, diagnosic symptor, alcohol, infection, cirrhosis and survival) and the risk model in E-MTAB-6389 dataset by comparing the risk score under different clinical information.

2.6. Clinical nomogram model

RiskScore, gender, vascular lnvasio, necrosis, diagnosic symptor, alcohol, and cirrhosis were enrolled into univariate and multivariate Cox analysis to authenticate independent prognostic predictors. The 'rms' package was employed to create a nomogram incorporating prognostic genes, enabling the prediction of CHOL patient survival. Evaluation of the predictive capacity was conducted through calibration curve analysis.

2.7. Functional enrichment analysis

Likewise, the 'limma' package was utilized to calculate the DEGs between two risk subgroups (adjusted P.value < 0.05). Then, GO and KEGG was applied to show the function of DEGs.

2.8. Immune feature estimation and chemotherapy analysis

We used single sample gene set enrichment analysis (ssGSEA) algorithm to calculate the expression status of 28 immune cells infiltrated in CHOL microenvironment. Specifically, we used a background reference gene set of 28 immune cells for ssGSEA immune infiltration analysis. These gene sets were obtained from the published literature and we used log2 normalization during data processing [22]. Following that, correlation coefficients between immune cells and prognostic genes were computed and Spearman's correlation analysis between risk scores and immune cells was performed. Using the 'ggplot2' package, the expression of some immune checkpoints within two risk-groups was analyzed. We further analyzed the difference in Tumor Immune Dysfunction and Exclusion (TIDE) scores between high and low risk groups. Finally, the half inhibitory concentration (IC50) of several drugs for each CHOL sample was calculated by pRRophetic package [23].

2.9. Statistic analysis

Analyses of public data were performed using the R programming language, and differential analysis comparisons were performed using the Wilcox test. All results were considered statistically significant when $P < 0.05$.

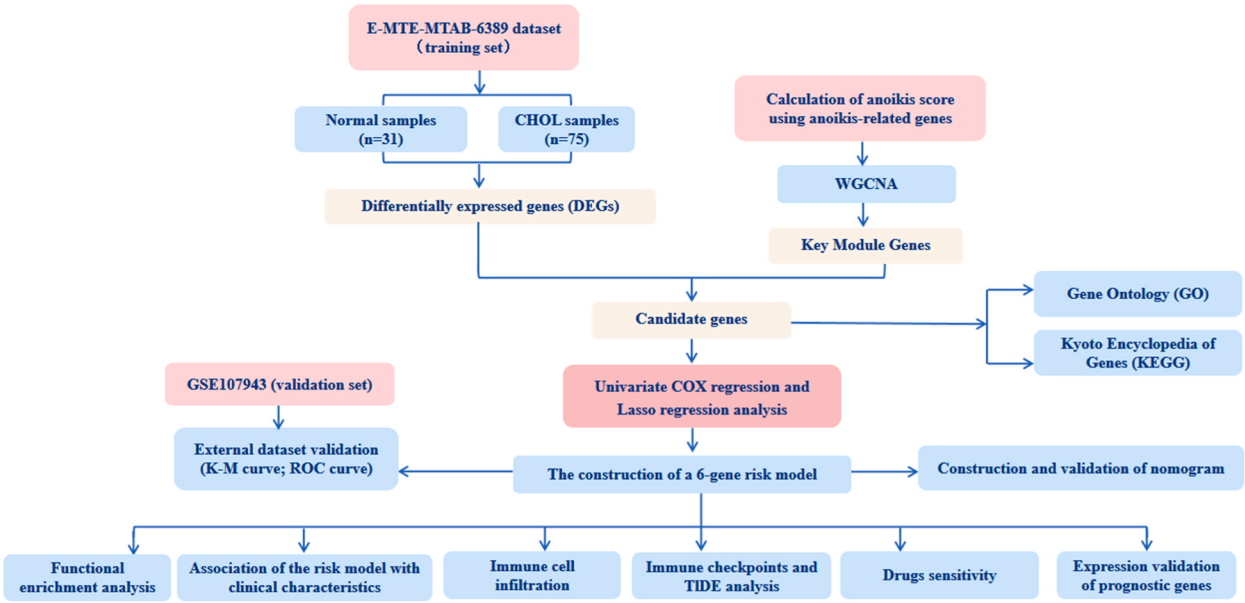

Fig. 1. Flow chart of the study.

3. Results

3.1. Identification of DEGs and module genes related to anoikis in CHOL

The flowchart of the study was presented in Fig. 1. 1844 DEGs were identified in CHOL, 982 of which were down-regulated and 862 of which were up-regulated (Fig. 2A). We selected the top 10 down-regulated and top 10 up-regulated genes to display in heatmap (Fig. 2B). To seek out key modules linked to anoikis, we carried out a WGCNA. There were no outlier samples, according to sample clustering data (Fig. 2C). The optimal soft threshold was 3. As the mean connectivity tended towards 0, the ordinate scale-free fit index, signed R^2 approached the critical value of 0.85 (red line) (Fig. 2D). The sample and trait heat map were shown in Fig. 2E. The dynamic tree cut algorithm yielded a total of 7 modules (Fig. 2F). And then, MEblack and MEturquoise module were markedly correlated with anoikis (Fig. 2G). Thus, 2678 key module genes related to anoikis were obtained (|GS| > 0.2, |MM| > 0.5). Furthermore, 1270 anoikis-

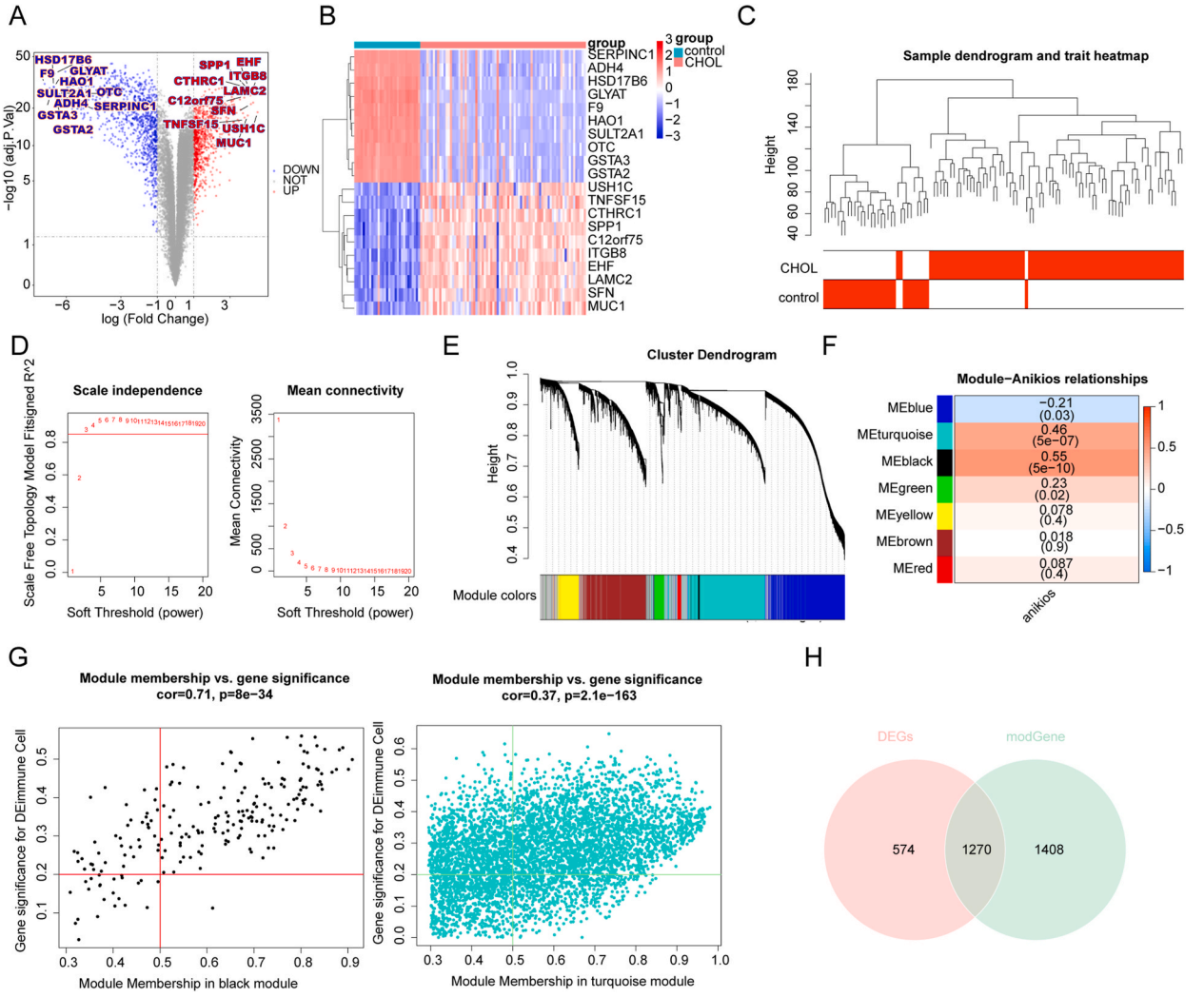

Fig. 2. Identification of DEGs and module genes related to anoikis in CHOL. (A) Heatmap and (B) volcano plot of differentially expressed genes in CHOL. (C) Sample clustering tree. (D) Screening of the soft threshold power. Scale independence (left). Mean connectivity (right). The horizontal axes are all soft thresholds, the vertical axis of the left figure is the scale free topological model fitting index, and the vertical axis of the right figure is the mean connectivity. (E) Hierarchical clustering tree. Different colors are used below to distinguish different modules, and above are the results of gene clustering. (F) Heatmap of module-trait correlations. The horizontal axis is the anoikis score, the vertical axis is the different modules, and the main part is the correlation heat map, with blue indicating negative correlation and red indicating positive correlation. In each corresponding individual grid, the value is the correlation coefficient. The larger the absolute value of the coefficient, the stronger the correlation. The median significance *P* value in the brackets. The smaller the *P* value, the more significant the result. (G) Screening of key module genes. MEblack filtered results (left). MEtruquoise filtered results (right). (H) The intersection of the differential genes in CHOL and the key module genes of anoikis was visualized by Venn diagram. (For interpretation of the references to color in this figure legend, the reader is referred to the Web version of this article.)

related differential genes (AKR-DEGs) were obtained (Fig. 2H). In addition, the functional enrichment analysis was performed. The GO analyses indicated their primary involvement in the small molecule catabolic process and organic acid catabolic process (Fig. 3A). However, we found that extracellular matrix-related structures were enriched in cellular component (CC), and we speculated the corresponding function of the extracellular matrix was likely to be related to anoikis. The KEGG analysis suggested that a predominant

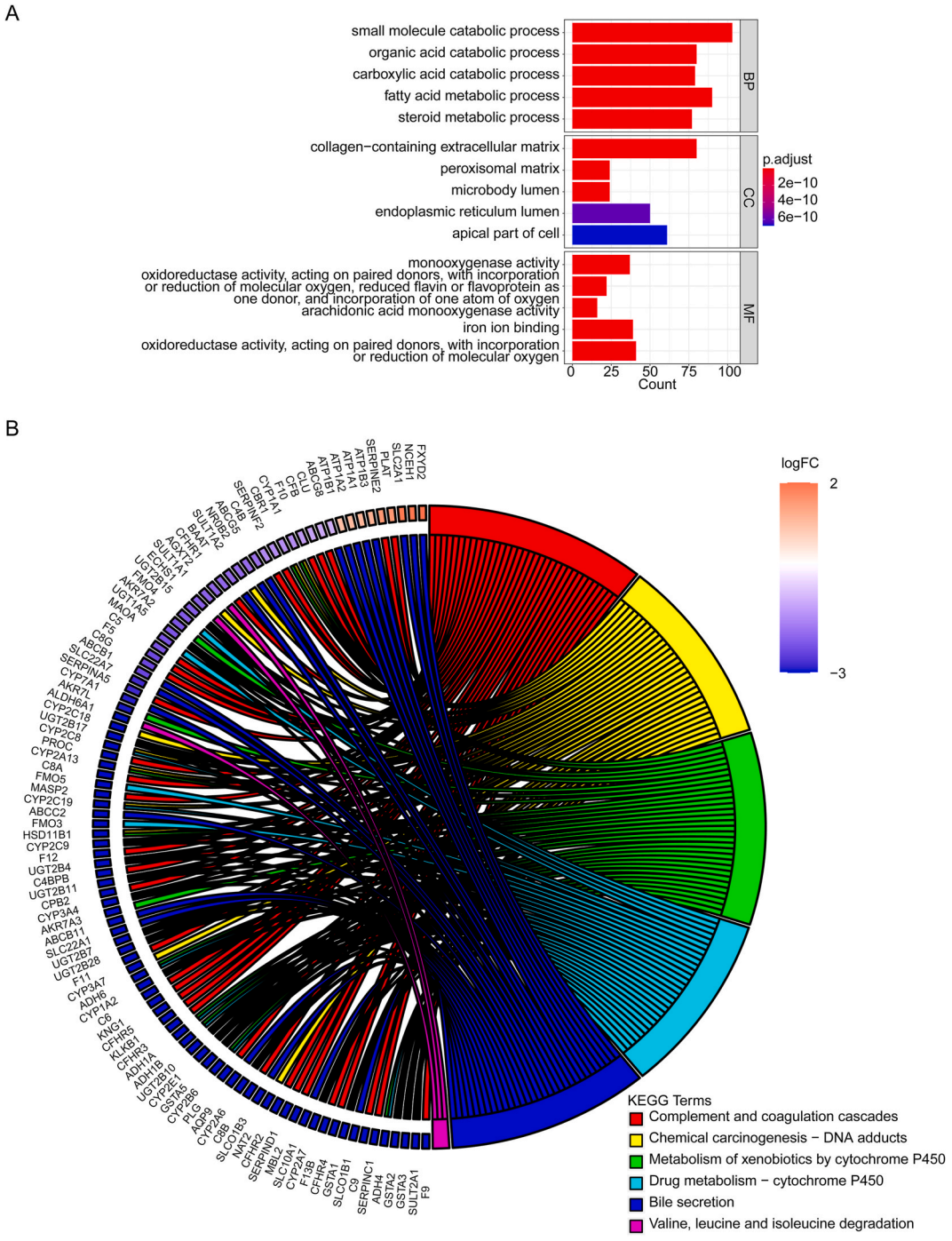

Fig. 3. Functional enrichment analysis of 1270 anoikis-related differential genes (AKR-DEGs). (A) GO enrichment bar plot. The horizontal axis is the number of genes enriched in GO entries, and the vertical axis is the corresponding entry name. The red-blue gradient represents the change in the significance *P* value. The smaller the value, the more significant the result. (B) KEGG chord diagram. Different colors distinguish different KEGG entries, and gene names are enriched to the corresponding pathways. $P < 0.05$ is considered to be statistically significant. (For interpretation of the references to color in this figure legend, the reader is referred to the Web version of this article.)

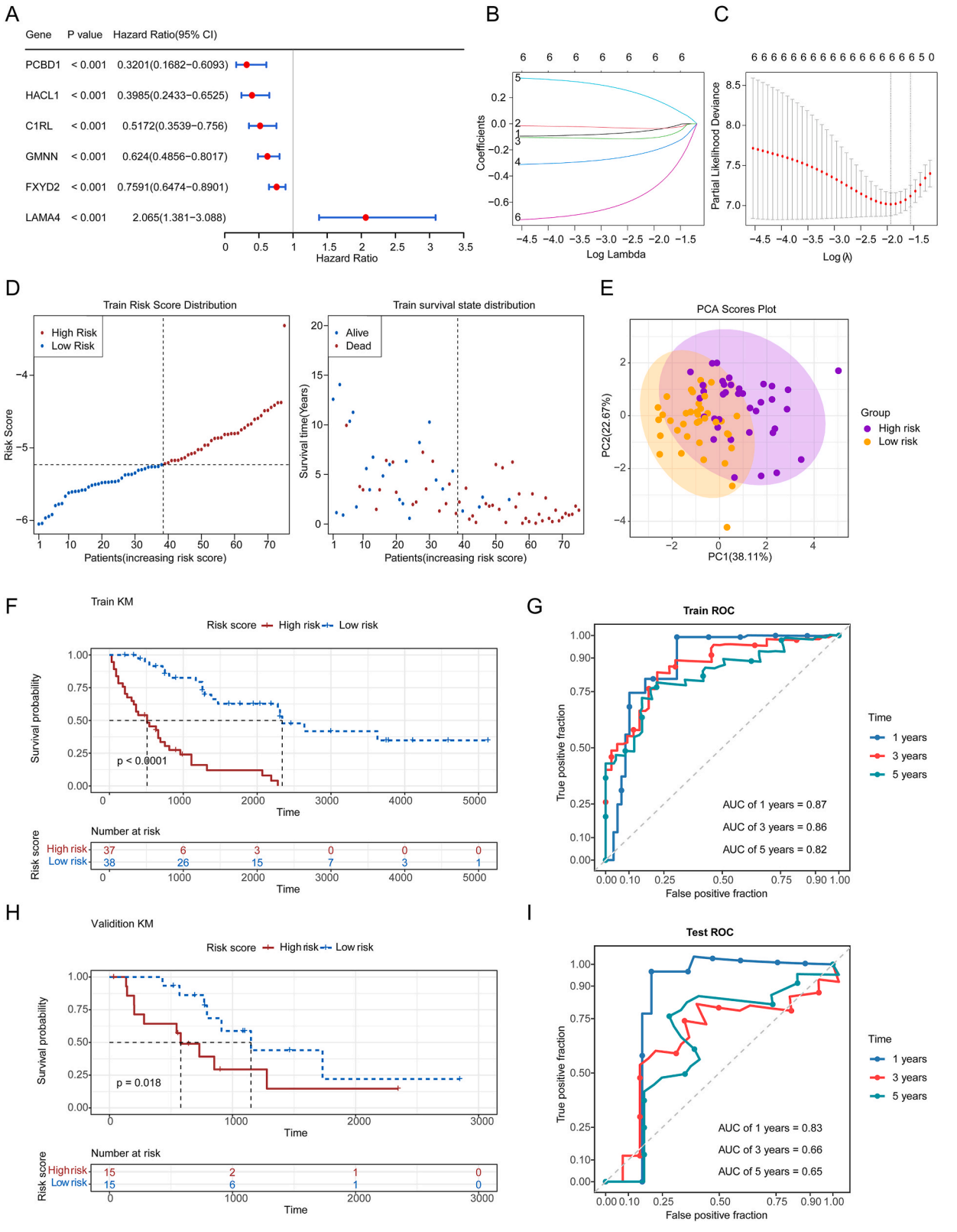

(caption on next page)

Fig. 4. Evaluation and validation of anoikis-related genes signature in training set and validation set. (A) Univariate cox forest plot showed 6 genes related to prognosis. (B–C) The LASSO Cox regression model to identify the most robust anoikis-related signatures. (D) Distribution of the risk score (left) and the survival status (right) in training set. (E) PCA scatter plot. (F) K-M curves for OS in training set. (G) Time-dependent ROC curves at 1- 3- and 5- year for OS in training set. (H) K-M curves for OS in validation set. (I) Time-dependent ROCcurves at 1- 3- and 5- year for OS in validation set. $P < 0.05$ is considered to be statistically significant.

enrichment of AKR-DEGs within the cytochrome P450 pathway (Fig. 3B).

3.2. Prognostic signature based on AKR-DEGs

Univariate Cox regression analysis and LASSO regression analysis and LASSO algorithm were utilized for excavate prognostic DEGs in E-MTAB-6389 dataset (Fig. 4A–C). Finally, we discovered 6 genes: FXYD Domain Containing Ion Transport Regulator 2 (*FXYD2*), Pterin-4 Alpha-Carbinolamine Dehydratase 1 (*PCBD1*), Complement C1r Subcomponent Like (*C1RL*), Geminin DNA Replication Inhibitor (*GMNN*), Laminin Subunit Alpha 4 (*LAMA4*) and 2-Hydroxyacyl-CoA Lyase 1 (*HACL1*). They were selected as prognostic anoikis-related genes for building a prognostic signature. Then, the CHOL patients were segregated into two risk groups: high and low risk (Fig. 4D). Principal components analysis (PCA) result indicated that six prognostic genes could distinguish two risk subgroups (Fig. 4E). Significantly, we observed notable survival discrepancies between the two risk groups, with patients in the high-risk CHOL group exhibiting poorer survival rates (Fig. 4F). For further assessment of the model's reliability, the Area Under Curve (AUC) of the model in forecasting 1-, 3-, 5-year survival of CHOL patients was 0.87, 0.86, and 0.82 in the EMBL-EBI database, indicating the risk model can forecast the survival outcomes of CHOL patients (Fig. 4G). Next, we further validated the risk model in the external validation dataset (GSE107943). In line with the results generated from the E-MTAB-6389 dataset, CHOL patients in high-risk group had awful OS (Fig. 4H). AUC of the 1 -, 3 - and 5-year was basically greater than 0.6 (Fig. 4I).

3.3. Independent prognostic analysis for CHOL patients

By comparing risk scores for subgroups with different clinicopathological features, we observed a significant difference in the risk scores concerning survival outcomes. (Fig. 5A). The results of Cox analysis demonstrated that both alcohol consumption and the risk score functioned as independent prognostic factors ($P < 0.05$) (Fig. 5B–C). The nomogram was generated, and the calibration curves confirmed the efficacy of the risk model's performance (Fig. 5D–E).

3.4. Analysis of immune infiltration and therapy

We obtained 105 DEGs in two risk groups through differential analysis, including 66 down-regulated and 39 up-regulated genes (Fig. 6A). We selected the top 10 down-regulated and top 10 up-regulated genes to display in heatmap (Fig. 6B). Furthermore, the GO analyses highlighted that these genes primarily functioned within the extracellular matrix (Fig. 6C). The KEGG results indicated that these genes were predominantly associated with the apoptosis pathway and Mucin type O-glycaan biosynthesis pathway (Fig. 6D). We then analyzed the expression status of 28 types of immune cells (Fig. 6E). Remarkably, seven immune cell abundances exhibited significant differences, including central memory CD4+T cell, central memory CD8+T cell, effector memory CD8+T cell, Myeloid-derived suppressor cells (MDSCs), plasmacytoid dendritic cells (pDCs), regulatory T cells (Tregs) and Type2 T helper (Th2) cell. We conducted further analysis to examine the correlation between prognostic genes and the scores of 28 immune cell types (Fig. 6F). In addition, we found a strong correlation between Activated dendritic cell and risk scores (Fig. S1). We found a negative correlation between *FXYD2*, *PCBD1*, *GMNN* and immune cells, while *LAMA4*, *C1RL*, *HACL1* were positively correlated with immune cells. Additionally, we assessed the variations in expression among some immune checkpoint molecules (Fig. 7A). Pearson correlation analysis revealed that Galectin 9 (*LAGLS9*) and Programmed Cell Death 1 Ligand 2 (*PDCD1LG2*) showed a notable positive correlation with the risk scores (Fig. 7B). We further found no significant difference in TIDE scores in the high-low risk group, suggesting that immune checkpoint blockade (ICB) therapy may be of little significance to the risk model (Fig. 7C). Furthermore, we conducted an analysis on the IC50 difference of several drugs which were frequently used in cancer between two subgroups (Fig. 7D). The results showed that the low-risk group had a higher response to Bosutinib, Gefitinib, Gemcitabine, and Paclitaxel while the high-risk group had a better response to Axitinib, Cisplatin, and Imatinib.

3.5. Expression validation of prognostic genes

The expression patterns of prognostic genes were separately analyzed within both the training and validation sets. We discovered that the expression value of *C1RL*, *HACL1* and *PCBD1* in the normal group were higher than those detected in the CHOL group. However, *FXYD2*, *GMNN* and *LAMA4* showed the opposite trend (Fig. 8A–B).

4. Discussion

As a malignancy with a poor prognosis, a critical need exists for research into novel molecular biomarkers associated with the treatment and personalized prognosis prediction of CHOL patients. Anoikis is an apoptotic process as a result of loss or improper cell

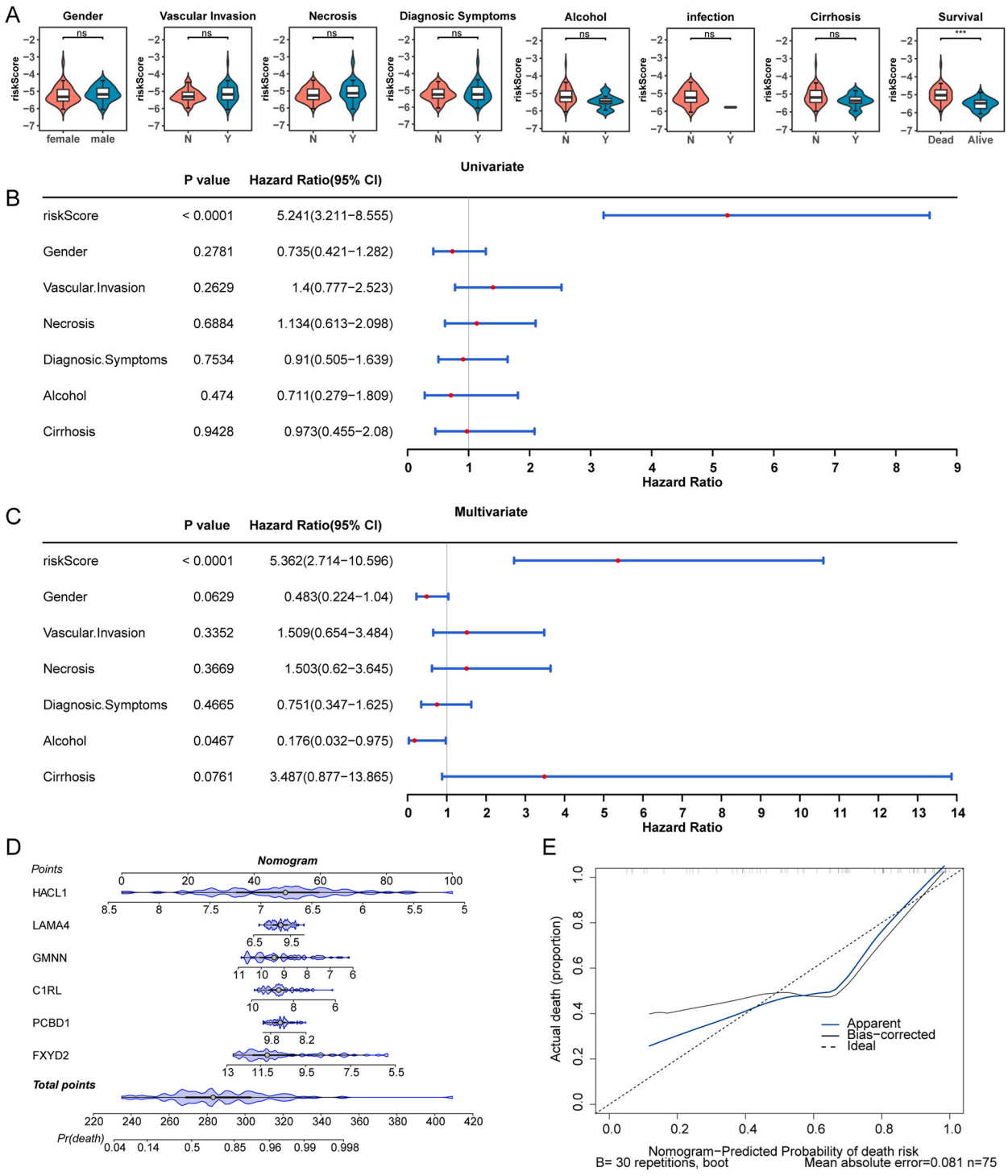

Fig. 5. Independent prognostic analysis for CHOL patients. (A) Distribution of risk scores for different clinical indicators. From left to right and top to bottom: gender, vascular invasion, necrosis, diagnostic symptoms, alcohol consumption, infection, cirrhosis, and survival. N means the feature is absent, Y means the feature is present. Univariate (B) and multivariate (C) Cox regression analyses to assess the relationship between the riskScore and clinical indicators and OS in the training set. (D) Predicting survival probability by building a nomogram using ARGs. (E) Nomogram calibration curve. The horizontal axis represents the death risk predicted by the nomogram, and the vertical axis represents the actual death. $^{*}P < 0.05$, $^{**}P < 0.01$, $^{***}P < 0.001$, $^{****}P < 0.0001$, *ns*: The difference is not significant.

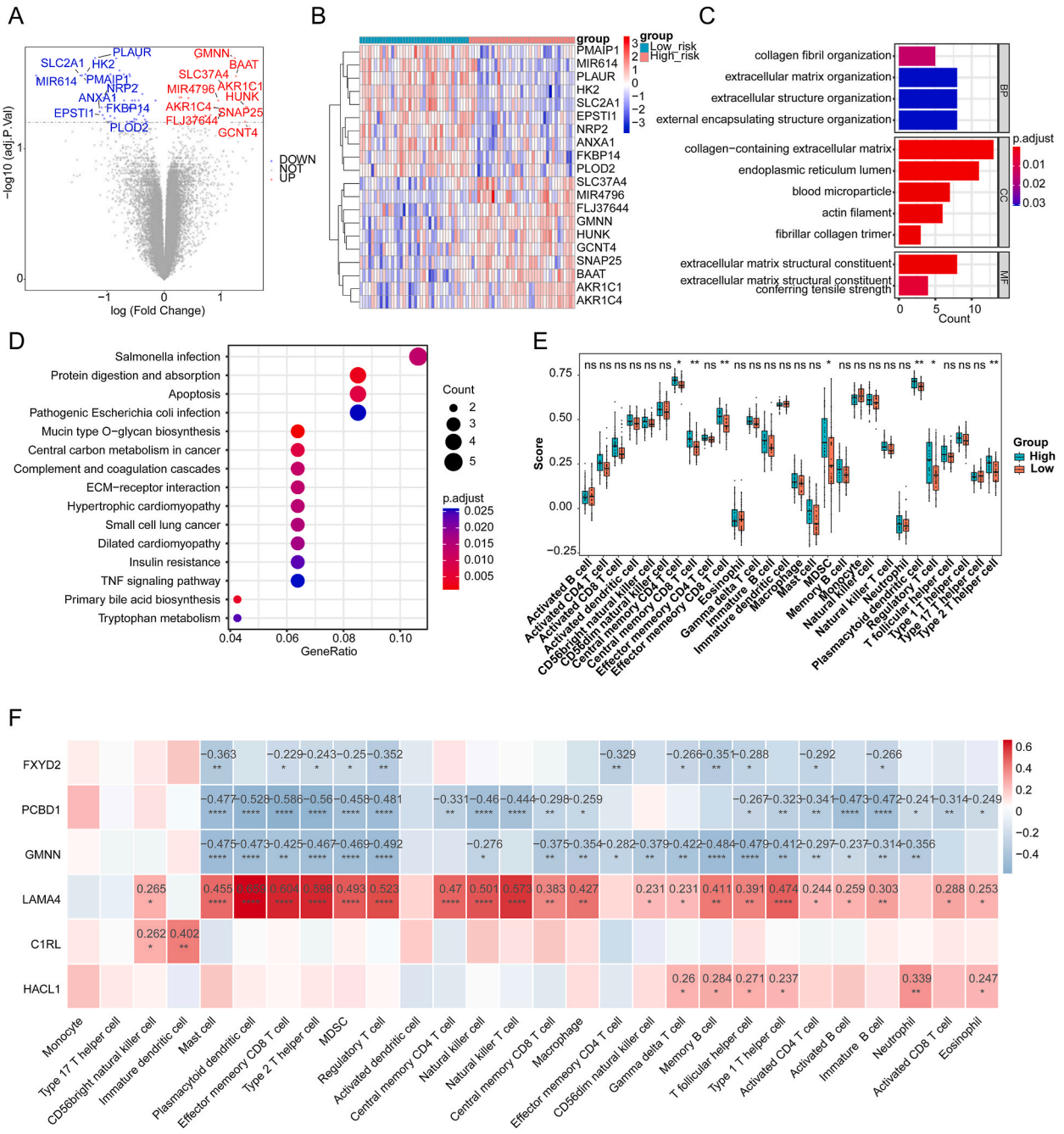

Fig. 6. Functional enrichment and immune infiltration analysis of differential genes between high and low risk groups. (A) Volcano plot and (B) heatmap of differentially expressed genes in different risk groups. (C) GO enrichment bar plot. (D) KEGG enrichment bubble plot. (E) Differential immune cell identification in high-risk and low-risk groups. (F) Correlation analysis between ARGs and immune cell infiltration. $^{*}P < 0.05$, $^{**}P < 0.01$, $^{***}P < 0.001$, $^{****}P < 0.0001$, *ns*: The difference is not significant.

adhesion [24]. It is commonly dysregulated in a range of illnesses and ensures physiologically relevant processes of development and tissue homeostasis [25]. In order to prevent apoptosis and preserve pro-survival signals, cancer cells exhibit deregulation of anoikis execution, which also facilitates the growth of distant organ metastases [26]. Anoikis resistance is also responsible for treatment failure in many cancers. Therefore, it is essential to investigate the worth of ARGs in CHOL in order to improve the prognosis of patients.

In this study, we first discovered 1270 ARGs differentially expressed in CHOL using public database data and WGCNA. Then, the Cox and Lasso regression models were used to further screen out 6 ARGs related to prognosis, and a prognosis prediction signature based on the 6 ARGs was constructed. And we used gene expression to construct a nomogram that has aided in prognostic prediction.

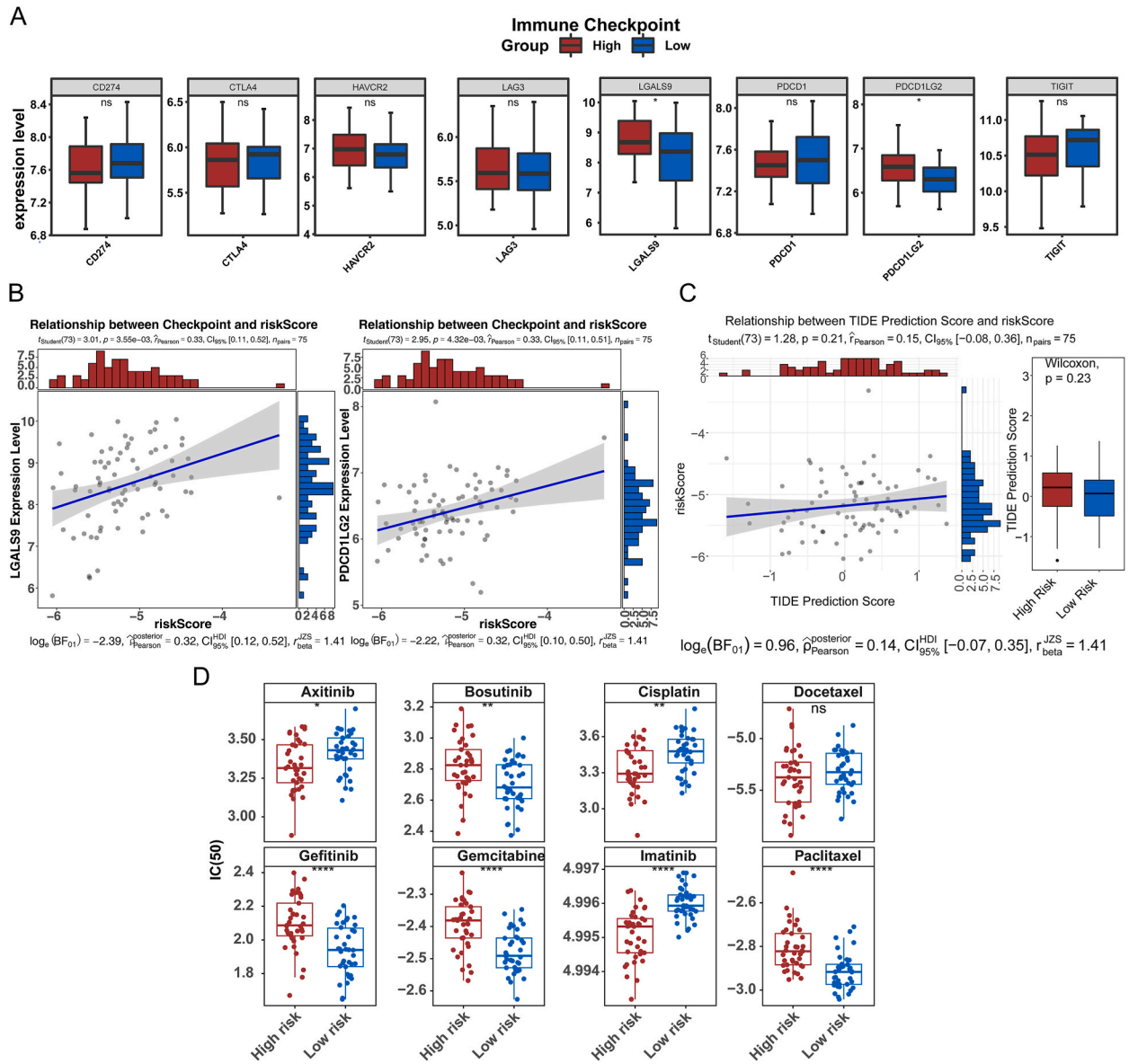

Fig. 7. Analysis of risk scores and immunotherapy and drug therapy. (A) Box plot showed the correlation between common immune checkpoints and risk scores. (B) Correlation analysis of differential immune checkpoints (LAGLS9, PDCD1LG2) with risk scores. (C) TIDE analysis results. Scatter plot of correlation between riskScore and TIDE prediction score (left). Analysis of differences in TIDE prediction score between high and low risk groups (right). (D) Boxplots showed the difference in IC50 values of Axitinib, Bosutinib, Cisplatin, Docetaxel, Gefitinib, Gemcitabine, Imatinib and Paclitaxel in different risk groups. *$P < 0.05$, **$P < 0.01$, ***$P < 0.001$, ****$P < 0.0001$, *ns*: The difference is not significant.

We also researched the relationship between immune cells, immune checkpoints, and immunotherapy and drug therapy in relation to risk scores.

Interestingly, we found that the underlying functions of ARGs were diverse; for instance, mutations causing hyperphenylalaninemia, hypomagnesemia, and diabetes have been linked to *PCBD1*, a gene that encoded a moonlighting protein [27]. It was reported that *PCBD1* was involved in hepatocellular carcinoma progression as it regulated the dimerization of HIF1-α and increased the transcriptional potency of HIF1-α [28]. In addition, studies have demonstrated that HNF1β-mediated *FXYD2* promoter activation was increased in the presence of *PCBD1* [29]. *PCBD1* might be involved in the development of CHOL by enhancing the activity of FXYD. One of the transmembrane proteins belonging to the FXYD family, which was primarily engaged in controlling Na+/K + -ATPase, was encoded by the gene *FXYD2*. This protein might also participated in the development of tumors [30]. Studies have shown that Na+/K + -ATPase was a target in the induction process of epithelial-to-mesenchymal transition (EMT) mediated by transforming growth factor (TGF)-β1 [31], and the activation of EMT was often beneficial to the anoikis resistance of tumors [32]. We speculated that *FXYD2* affected EMT and anoikis resistance by regulating Na+/K + -ATPase, thus improving the prognosis of CHOL.

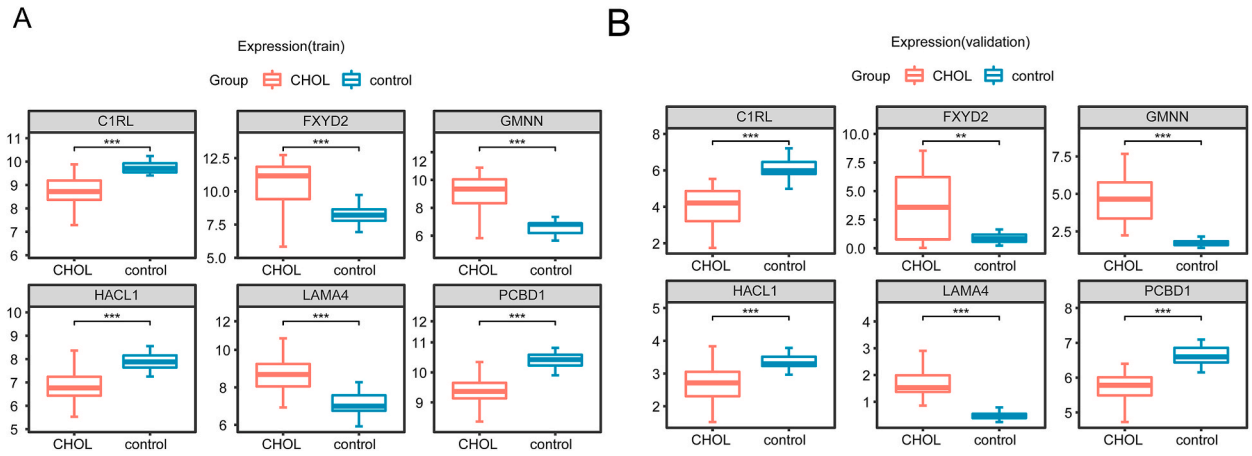

Fig. 8. Expression validation of prognostic genes. (A) Boxplots showed differences in expression levels of prognostic genes in the training set. (B) Boxplots showed differences in expression levels of prognostic genes in the validation set. *$P < 0.05$, **$P < 0.01$, ***$P < 0.001$, ****$P < 0.0001$, *ns*: The difference is not significant.

Through sequencing analysis, we discovered that increased expression of *PCBD1* and *FXYD2* was linked to a better prognosis, which might be confirmed this speculation. *GMNN* was responsible for producing a protein that was crucial for the regulation of the cell cycle. Researchers have found that *GMNN* acted as a suppressor of tumors by preserving genome stability, but its over-expression was related to genome instability and was considered an oncogene [33]. It has been shown that *GMNN* is involved in ATM/ATR and p53-mediated DNA repair, cell cycle and apoptosis [34]. As an indicator of the proliferation of cells, *GMNN* has been reported to be linked to apoptosis regulation, including Bcl2 and activated caspase-3 [34], which were important players in the anoikis pathway [26]. In our study, its expression increased in CHOL and it was considered to be a protective gene. It might promote tumor anoikis by regulating apoptotic molecule in CHOL and we will maintain our focus on studying the role of this gene in the future.

As for *C1RL*, which was responsible for facilitating the proteolytic cleavage of HP/haptoglobin within the endoplasmic reticulum [35]. In molecular role, *C1RL* protein acts as the active form of a serine hydrolase [36]. Studies have shown that *C1RL* expression in glioblastoma was associated with decreased tumor purity and higher infiltration of M2 macrophage, which was related to poor prognosis [37]. In renal cell carcinoma [38], *C1RL* was considered to be involved in its occurrence and development, but in hepatocellular carcinoma [39], notably, patients with high *C1RL* expression has a better prognosis. In addition, *C1RL* was found to be a protective gene in CHOL in our study, and it was positively correlated with immune cell abundance. We speculated that it had the potential to improve patient outcomes by regulating the immune response. *HACL1* was an essential enzyme in the peroxisomal α-oxidation of phytanate [40]. It had been reported that *HACL1* might take part in hepatic cholestasis through the signaling pathway connected to PPAR-α [41]. Our study found that decreased expression of *HACL1* in patients with CHOL was associated with worse prognosis. However, the exact mechanism of action needs more explorations, we will continue to focus on the function of this gene in the future. A laminin family member, *LAMA4* was abundantly distributed in the basement membranes of many organs [42]. There is ample evidence linking it to the emergence of various cancers. For instance, the elevated level of *LAMA4* was indicative of liver cancer invasion and metastasis [43]. In renal cell carcinoma, *LAMA4* promoted tumor cell migration by inducing the expression of integrin α5β1 through the ILK/FAK/ERK pathway [44]. Notably, the development of EMT in oral squamous cell carcinoma results in a switch from laminin α5 chain production to laminin α4 chain synthesis, which enables the tumor cells to break free from strong adherence to the extracellular matrix or basement membrane [45]. Our research findings also demonstrated that *LAMA4* was a substantial risk element for CHOL, and patients with higher *LAMA4* expression tended to have a worse prognosis. This elevated *LAMA4* expression might facilitate the resistance to anoikis by triggering changes in integrins and promoting EMT.

To explore the underlying functions or mechanisms of gene signatures in CHOL, we conducted functional enrichment analysis. KEGG enrichment analysis showed that the selected genes were mostly enriched in apoptosis, mucin O-type-glycan biosynthesis, ECM-receptor interaction, TNF signaling pathway, etc. First, abnormal apoptosis often leads to the occurrence of cancer. Apoptosis relies on the activation of different signaling pathways, but these signaling pathways were often dysregulated in cancer [46]. Secondly, abnormalities in mucin O-type-glycan were considered to be a crucial element in the emergence of epithelial diseases. In tumors, they were often accompanied by changes in the structure and quantity of mucin O-type-glycan, forming tumor-specific glycan structures [47]. Their imbalance offers molecular insights into the initiation and advancement of cancer [48]. In addition, TNF was tumor necrosis factor, which was considered a cytokine with well-known anti-cancer properties [49]. Studies have shown that TNF family members were related to angiogenesis in CHOL [50].

There is no doubt that the tumor microenvironment plays a major role in the pathogenesis of cancer, so we further investigated the relation between risk scores and immune infiltration. We discovered that CHOL patients in the high-risk group had higher tumor immune cell infiltration. Although central and effector memory CD4/CD8+T cells were thought to exert anti-tumor effects [51], it seemed plausible that patients in the high-risk group had an immune milieu with a stronger tumor-suppressive response. For instance, MDSCs were believed to play a role not only in directly facilitating immune evasion but also in fostering tumor invasion through

various non-immune mechanisms [52]. Studies have shown that high abundance of pDC in the tissue surrounding iCCA tumors was related to shorter OS and greater likelihood of recurrence, and pDC infiltration might indicate immune tolerance in the peritumoral microenvironment [53].

And it was reported that the cancer cells secrete TGF-β1, leading to the induction of Tregs in biliary tract cancer, thus establishing an immune-suppressive microenvironment and supporting progression of tumors [54]. In addition, Th2-related mast cells were considered pertinent players in CHOL formation and might facilitate tumor growth by acting as promoters of angiogenesis [55]. Furthermore, although TIDE scores did not differ across the risk groups, but we found that *LAGLS9* and *PDCD1LG2* were highly expressed in the high-risk group in CHOL and were positively linked to the risk score. According to reports, *LGALS9* binds to Tim-3 and induces apoptosis by inducing T-helper 1 cell death via intracellular calcium current. Thus, this leads to induction of immune tolerance and inhibition of T-helper 1 and T-helper 17 cells responses [56]. It was demonstrated that inhibiting the *LGALS9*/Tim-3 pathway elicits anti-tumor immune responses and hampers the development of tumors [57]. Additionally, it has been indicated that binding of *PDCD1LG2* to PD-1 significantly inhibits T cell receptor-mediated proliferation and cytokine production by T cells [58]. Tanegashima et al. [59] indicated that the expression of *PDCD1LG2* in tumor cells played a crucial role in evading anti-tumor immunity. The abnormal expression of these two immune checkpoints in CHOL might be beneficial to tumor immune evasion and might be used as potential immunotherapy targets for subsequent research.

Furthermore, we evaluated the significance of the anoikis-related gene signature in terms of drug sensitivity. We found that the low-risk patients were more sensitive to Bosutinib, Gefitinib, Gemcitabine, and Paclitaxel, while the high-risk group showed greater sensitivity to Axitinib, Cisplatin, and Imatinib. Gemcitabine was a cell cycle-specific chemotherapeutic agent whose cytotoxic effect lied in the inhibition of DNA synthesis. Studies have shown that its combination with cisplatin has become the first-line chemotherapy regimen for CHOL [60]. Considering the results above, the construction of the signature is beneficial to guide the selection of clinical medications.

In summary, this study was the first to explore the prognostic value of ARGs in CHOL and create a signature of anoikis-related prognostic genes. This signature performed well in predictions and can be used to create individualized treatment plans for CHOL patients. In light of the limited existing research in this domain, our study not only provided fresh insights and avenues for future investigation regarding anoikis in CHOL but also served as a pivotal reference point for the exploration of innovative therapeutic approaches. These findings expand our understanding of the prognostic value in CHOL, bolstering the advancement of personalized medicine and precision healthcare. However, it is important to acknowledge the limitations inherent in our research. One key limitation is that our results are primarily based on data obtained from public databases, which may vary in terms of quality, consistency, and reliability. Thus it can lead to results that can overlap like survival analysis. Finally, this study has not yet fully elucidated the effect of ARGs on anoikis and the regulatory mechanism of CHOL, and further experimental research is needed to explore it. We will continue to monitor the role of these genes.

Funding statement

Not applicable.

Ethics approval and consent to participate

Not applicable.

Consent for publication

Not applicable.

Data availability statement

E-MTAB-6389 dataset analyzed for this study was collected from EMBL-EBI database; GSE107943 datasets analyzed for this study can be found in the GEO database (http://www.ncbi.nlm.nih.gov/geo/).

CRediT authorship contribution statement

Guochao Liu: Writing – original draft, Visualization, Methodology, Formal analysis, Conceptualization. **Yujian He:** Writing – original draft, Visualization, Methodology, Formal analysis, Data curation. **Zhaoqiang Yin:** Writing – review & editing, Project administration, Conceptualization. **Zhijie Feng:** Writing – review & editing, Validation, Supervision.

Declaration of competing interest

The authors declare that they have no known competing financial interests or personal relationships that could have appeared to influence the work reported in this paper.

Acknowledgements

We express our gratitude to all of the participants in the study.

Appendix A. Supplementary data

Supplementary data to this article can be found online at https://doi.org/10.1016/j.heliyon.2024.e32337.

References

[1] Z.W. Meng, L. Zhang, X.R. Cai, X. Wang, F.F. She, Y.L. Chen, IL-8 is a novel prometastatic chemokine in intrahepatic cholangiocarcinoma that induces CXCR2-PI3K/AKT signaling upon CD97 activation, Sci. Rep. 13 (1) (2023) 18711, https://doi.org/10.1038/s41598-023-45496-3.
[2] L.N.C. Boyd, L.E. Nooijen, M. Ali, J.R. Puik, J. Moustaquim, S.M. Fraga Rodrigues, R. Broos, A. Belkouz, L.L. Meijer, T.Y.S. Le Large, J.I. Erdmann, G.K. J. Hooijer, M. Heger, H.W.M. Van Laarhoven, E. Roos, G. Kazemier, E. Giovannetti, J. Verheij, H.J. Klümpen, Prognostic and predictive value of human equilibrative nucleoside transporter 1 (hENT1) in extrahepatic cholangiocarcinoma: a translational study, Front. Pharmacol. 14 (2023) 1274692, https://doi.org/10.3389/fphar.2023.1274692.
[3] Q. Sun, H. Wang, B. Xiao, D. Xue, G. Wang, Development and validation of a 6-gene hypoxia-related prognostic signature for cholangiocarcinoma, Front. Oncol. 12 (2022) 954366, https://doi.org/10.3389/fonc.2022.954366.
[4] J. Wang, S. Ilyas, Targeting the tumor microenvironment in cholangiocarcinoma: implications for therapy, Expet Opin. Invest. Drugs 30 (4) (2021) 429–438, https://doi.org/10.1080/13543784.2021.1865308.
[5] Z. Wang, X. Chen, Z. Jiang, Immune infiltration and a ferroptosis-related gene signature for predicting the prognosis of patients with cholangiocarcinoma, Am J Transl Res 14 (2) (2022) 1204–1219.
[6] Y. Wang, S. Chen, S. He, Bioinformatics analysis of inflammation gene signature in indicating cholangiocarcinoma prognosis, JAMA Oncol. 2022 (2022) 9975838, https://doi.org/10.1155/2022/9975838.
[7] H.J. Han, J.Y. Sung, S.H. Kim, U.J. Yun, H. Kim, E.J. Jang, H.E. Yoo, E.K. Hong, S.H. Goh, A. Moon, J.S. Lee, S.K. Ye, J. Shim, Y.N. Kim, Fibronectin regulates anoikis resistance via cell aggregate formation, Cancer Lett. 508 (2021) 59–72, https://doi.org/10.1016/j.canlet.2021.03.011.
[8] A.P. Gilmore, Anoikis, Cell Death Differ. 12 (Suppl 2) (2005) 1473–1477, https://doi.org/10.1038/sj.cdd.4401723.
[9] E. Kakavandi, R. Shahbahrami, H. Goudarzi, G. Eslami, E. Faghihloo, Anoikis resistance and oncoviruses, J. Cell. Biochem. 119 (3) (2018) 2484–2491, https://doi.org/10.1002/jcb.26363.
[10] F.O. Adeshakin, A.O. Adeshakin, L.O. Afolabi, D. Yan, G. Zhang, X. Wan, Mechanisms for modulating anoikis resistance in cancer and the relevance of metabolic reprogramming, Front. Oncol. 11 (2021) 626577, https://doi.org/10.3389/fonc.2021.626577.
[11] Z. Sun, Y. Zhao, Y. Wei, X. Ding, C. Tan, C. Wang, Identification and validation of an anoikis-associated gene signature to predict clinical character, stemness, IDH mutation, and immune filtration in glioblastoma, Front. Immunol. 13 (2022) 939523, https://doi.org/10.3389/fimmu.2022.939523.
[12] S. Chen, J. Gu, Q. Zhang, Y. Hu, Y. Ge, Development of biomarker signatures associated with anoikis to predict prognosis in endometrial carcinoma patients, JAMA Oncol. 2021 (2021) 3375297, https://doi.org/10.1155/2021/3375297.
[13] X. Diao, C. Guo, S. Li, Identification of a novel anoikis-related gene signature to predict prognosis and tumor microenvironment in lung adenocarcinoma, Thorac Cancer 14 (3) (2023) 320–330, https://doi.org/10.1111/1759-7714.14766.
[14] H. Chi, P. Jiang, K. Xu, Y. Zhao, B. Song, G. Peng, B. He, X. Liu, Z. Xia, G. Tian, A novel anoikis-related gene signature predicts prognosis in patients with head and neck squamous cell carcinoma and reveals immune infiltration, Front. Genet. 13 (2022) 984273, https://doi.org/10.3389/fgene.2022.984273.
[15] Z. Zhang, Z. Zhu, J. Fu, X. Liu, Z. Mi, H. Tao, H. Fan, Anoikis patterns exhibit distinct prognostic and immune landscapes in Osteosarcoma, Int. Immunopharm. 115 (2023) 109684, https://doi.org/10.1016/j.intimp.2023.109684.
[16] A. Liberzon, C. Birger, H. Thorvaldsdóttir, M. Ghandi, J.P. Mesirov, P. Tamayo, The Molecular Signatures Database (MSigDB) hallmark gene set collection, Cell Syst 1 (6) (2015) 417–425, https://doi.org/10.1016/j.cels.2015.12.004.
[17] A. Colaprico, T.C. Silva, C. Olsen, L. Garofano, C. Cava, D. Garolini, T.S. Sabedot, T.M. Malta, S.M. Pagnotta, I. Castiglioni, M. Ceccarelli, G. Bontempi, H. Noushmehr, TCGAbiolinks: an R/Bioconductor package for integrative analysis of TCGA data, Nucleic Acids Res. 44 (8) (2016) e71, https://doi.org/10.1093/nar/gkv1507.
[18] K. Ito, D. Murphy, Application of ggplot2 to pharmacometric graphics, CPT Pharmacometrics Syst. Pharmacol. 2 (10) (2013) e79, https://doi.org/10.1038/psp.2013.56.
[19] P. Langfelder, S. Horvath, WGCNA: an R package for weighted correlation network analysis, BMC Bioinf. 9 (2008) 559, https://doi.org/10.1186/1471-2105-9-559.
[20] G. Yu, L.G. Wang, Y. Han, Q.Y. He, clusterProfiler: an R package for comparing biological themes among gene clusters, OMICS 16 (5) (2012) 284–287, https://doi.org/10.1089/omi.2011.0118.
[21] R. Tibshirani, The lasso method for variable selection in the Cox model, Stat. Med. 16 (4) (1997) 385–395, https://doi.org/10.1002/(sici)1097-0258(19970228)16:4<385::aid-sim380>3.0.co;2-3.
[22] P. Charoentong, F. Finotello, M. Angelova, C. Mayer, M. Efremova, D. Rieder, H. Hackl, Z. Trajanoski, Pan-cancer immunogenomic analyses reveal genotype-immunophenotype relationships and predictors of response to checkpoint blockade, Cell Rep. 18 (1) (2017) 248–262, https://doi.org/10.1016/j.celrep.2016.12.019.
[23] P. Geeleher, N. Cox, R.S. Huang, pRRophetic: an R package for prediction of clinical chemotherapeutic response from tumor gene expression levels, PLoS One 9 (9) (2014) e107468, https://doi.org/10.1371/journal.pone.0107468.
[24] Y. Jiang, Y. Wang, Z. Wang, Y. Zhang, Y. Hou, X. Wang, Anoikis-related genes signature development for clear cell renal cell carcinoma prognosis and tumor microenvironment, Sci. Rep. 13 (1) (2023) 18909, https://doi.org/10.1038/s41598-023-46398-0.
[25] M.L. Taddei, E. Giannoni, T. Fiaschi, P. Chiarugi, Anoikis: an emerging hallmark in health and diseases, J. Pathol. 226 (2) (2012) 380–393, https://doi.org/10.1002/path.3000.
[26] P. Paoli, E. Giannoni, P. Chiarugi, Anoikis molecular pathways and its role in cancer progression, Biochim. Biophys. Acta 1833 (12) (2013) 3481–3498, https://doi.org/10.1016/j.bbamcr.2013.06.026.
[27] L.E. Tholen, C. Bos, P. Jansen, H. Venselaar, M. Vermeulen, J.G.J. Hoenderop, J.H.F. de Baaij, Bifunctional protein PCBD2 operates as a co-factor for hepatocyte nuclear factor 1β and modulates gene transcription, Faseb. J. 35 (4) (2021) e21366, https://doi.org/10.1096/fj.202002022R.
[28] T. Ishiyama, J. Kano, Y. Minami, T. Iijima, Y. Morishita, M. Noguchi, Expression of HNFs and C/EBP alpha is correlated with immunocytochemical differentiation of cell lines derived from human hepatocellular carcinomas, hepatoblastomas and immortalized hepatocytes, Cancer Sci. 94 (9) (2003) 757–763, https://doi.org/10.1111/j.1349-7006.2003.tb01515.x.
[29] S. Ferrè, J.H. de Baaij, P. Ferreira, R. Germann, J.B. de Klerk, M. Lavrijsen, F. van Zeeland, H. Venselaar, L.A. Kluijtmans, J.G. Hoenderop, R.J. Bindels, Mutations in PCBD1 cause hypomagnesemia and renal magnesium wasting, J. Am. Soc. Nephrol. 25 (3) (2014) 574–586, https://doi.org/10.1681/asn.2013040337.

[30] M. Jin, H. Zhang, J. Yang, Z. Zheng, K. Liu, Expression mode and prognostic value of FXYD family members in colon cancer, Aging (Albany NY) 13 (14) (2021) 18404–18422, https://doi.org/10.18632/aging.203290.
[31] S.A. Rajasekaran, T.P. Huynh, D.G. Wolle, C.E. Espineda, L.J. Inge, A. Skay, C. Lassman, S.B. Nicholas, J.F. Harper, A.E. Reeves, M.M. Ahmed, J.M. Leatherman, J.M. Mullin, A.K. Rajasekaran, Na,K-ATPase subunits as markers for epithelial-mesenchymal transition in cancer and fibrosis, Mol. Cancer Therapeut. 9 (6) (2010) 1515–1524, https://doi.org/10.1158/1535-7163.Mct-09-0832.
[32] Z. Cao, T. Livas, N. Kyprianou, Anoikis and EMT: lethal "liaisons" during cancer progression, Crit. Rev. Oncog. 21 (3–4) (2016) 155–168, https://doi.org/10.1615/CritRevOncog.2016016955.
[33] S. Champeris Tsaniras, M. Villiou, A.D. Giannou, S. Nikou, M. Petropoulos, I.S. Pateras, P. Tserou, F. Karousi, M.E. Lalioti, V.G. Gorgoulis, A.L. Patmanidi, G. T. Stathopoulos, V. Bravou, Z. Lygerou, S. Taraviras, Geminin ablation in vivo enhances tumorigenesis through increased genomic instability, J. Pathol. 246 (2) (2018) 134–140, https://doi.org/10.1002/path.5128.
[34] P.P. Kushwaha, K.C. Rapalli, S. Kumar, Geminin a multi task protein involved in cancer pathophysiology and developmental process: a review, Biochimie 131 (2016) 115–127, https://doi.org/10.1016/j.biochi.2016.09.022.
[35] C.A. Schaer, C. Owczarek, J.W. Deuel, S. Schauer, J.H. Baek, A. Yalamanoglu, M.P. Hardy, P.D. Scotney, P.M. Schmidt, M. Pelzing, P. Soupourmas, P.W. Buehler, D.J. Schaer, Phenotype-specific recombinant haptoglobin polymers co-expressed with C1r-like protein as optimized hemoglobin-binding therapeutics, BMC Biotechnol. 18 (1) (2018) 15, https://doi.org/10.1186/s12896-018-0424-3.
[36] M. Navarrete, J. Ho, O. Krokhin, P. Ezzati, C. Rigatto, M. Reslerova, D.N. Rush, P. Nickerson, J.A. Wilkins, Proteomic characterization of serine hydrolase activity and composition in normal urine, Clin. Proteonomics 10 (1) (2013) 17, https://doi.org/10.1186/1559-0275-10-17.
[37] J. Wang, L. Tong, G. Lin, H. Wang, L. Zhang, X. Yang, Immunological and clinicopathological characteristics of C1RL in 2120 glioma patients, BMC Cancer 20 (1) (2020) 931, https://doi.org/10.1186/s12885-020-07436-6.
[38] C. Chinello, M. Cazzaniga, G. De Sio, A.J. Smith, A. Grasso, B. Rocco, S. Signorini, M. Grasso, S. Bosari, I. Zoppis, G. Mauri, F. Magni, Tumor size, stage and grade alterations of urinary peptidome in RCC, J. Transl. Med. 13 (2015) 332, https://doi.org/10.1186/s12967-015-0693-8.
[39] B. Xu, W. Lv, X. Li, L. Zhang, J. Lin, Prognostic genes of hepatocellular carcinoma based on gene coexpression network analysis, J. Cell. Biochem. 120 (7) (2019) 11616–11623, https://doi.org/10.1002/jcb.28441.
[40] S. Mezzar, E. De Schryver, S. Asselberghs, E. Meyhi, P.L. Morvay, M. Baes, P.P. Van Veldhoven, Phytol-induced pathology in 2-hydroxyacyl-CoA lyase (HACL1) deficient mice. Evidence for a second non-HACL1-related lyase, Biochim. Biophys. Acta Mol. Cell Biol. Lipids 1862 (9) (2017) 972–990, https://doi.org/10.1016/j.bbalip.2017.06.004.
[41] J. Yao, J. Yan, J. Wu, J. Yu, B. He, X. Chen, Z. Chen, Predicting target genes of san-huang-chai-zhu formula in treating ANIT-induced acute intrahepatic cholestasis rat model via bioinformatics analysis combined with experimental validation, Evid Based Complement Alternat Med 2021 (2021) 5320445, https://doi.org/10.1155/2021/5320445.
[42] J.J. Yu, L.J. Zhang, C.C. He, Y.F. Cao, J. Yang, [Research progress on the role of laminin Subunit alpha 4 in diseases], Zhongguo Yi Xue Ke Xue Yuan Xue Bao 45 (1) (2023) 92–100, https://doi.org/10.3881/j.issn.1000.503X.14615.
[43] X. Huang, G. Ji, Y. Wu, B. Wan, L. Yu, LAMA4, highly expressed in human hepatocellular carcinoma from Chinese patients, is a novel marker of tumor invasion and metastasis, J. Cancer Res. Clin. Oncol. 134 (6) (2008) 705–714, https://doi.org/10.1007/s00432-007-0342-6.
[44] Y. Li, B. Guan, J. Liu, Z. Zhang, S. He, Y. Zhan, B. Su, H. Han, X. Zhang, B. Wang, X. Li, L. Zhou, W. Zhao, MicroRNA-200b is downregulated and suppresses metastasis by targeting LAMA4 in renal cell carcinoma, EBioMedicine 44 (2019) 439–451, https://doi.org/10.1016/j.ebiom.2019.05.041.
[45] M. Takkunen, M. Ainola, N. Vainionpää, R. Grenman, M. Patarroyo, A. García de Herreros, Y.T. Konttinen, I. Virtanen, Epithelial-mesenchymal transition downregulates laminin alpha5 chain and upregulates laminin alpha4 chain in oral squamous carcinoma cells, Histochem. Cell Biol. 130 (3) (2008) 509–525, https://doi.org/10.1007/s00418-008-0443-6.
[46] D. Kashyap, V.K. Garg, N. Goel, Intrinsic and extrinsic pathways of apoptosis: role in cancer development and prognosis, Adv Protein Chem Struct Biol 125 (2021) 73–120, https://doi.org/10.1016/bs.apcsb.2021.01.003.
[47] G.E. Cervoni, J.J. Cheng, K.A. Stackhouse, J. Heimburg-Molinaro, R.D. Cummings, O-glycan recognition and function in mice and human cancers, Biochem. J. 477 (8) (2020) 1541–1564, https://doi.org/10.1042/bcj20180103.
[48] V. Mohan, A. Das, I. Sagi, Emerging roles of ECM remodeling processes in cancer, Semin. Cancer Biol. 62 (2020) 192–200, https://doi.org/10.1016/j.semcancer.2019.09.004.
[49] L. Bertazza, S. Mocellin, The dual role of tumor necrosis factor (TNF) in cancer biology, Curr. Med. Chem. 17 (29) (2010) 3337–3352, https://doi.org/10.2174/092986710793176339.
[50] S. Bakrim, N. Benkhaira, I. Bourais, T. Benali, L.H. Lee, N. El Omari, R.A. Sheikh, K.W. Goh, L.C. Ming, A. Bouyahya, Health benefits and pharmacological properties of stigmasterol, Antioxidants 11 (10) (2022), https://doi.org/10.3390/antiox11101912.
[51] S. Caserta, J.G. Borger, R. Zamoyska, Central and effector memory CD4 and CD8 T-cell responses to tumor-associated antigens, Crit. Rev. Immunol. 32 (2) (2012) 97–126, https://doi.org/10.1615/critrevimmunol.v32.i2.10.
[52] K. Li, H. Shi, B. Zhang, X. Ou, Q. Ma, Y. Chen, P. Shu, D. Li, Y. Wang, Myeloid-derived suppressor cells as immunosuppressive regulators and therapeutic targets in cancer, Signal Transduct. Targeted Ther. 6 (1) (2021) 362, https://doi.org/10.1038/s41392-021-00670-9.
[53] Z.Q. Hu, Z.J. Zhou, C.B. Luo, H.Y. Xin, J. Li, S.Y. Yu, S.L. Zhou, Peritumoral plasmacytoid dendritic cells predict a poor prognosis for intrahepatic cholangiocarcinoma after curative resection, Cancer Cell Int. 20 (1) (2020) 582, https://doi.org/10.1186/s12935-020-01676-z.
[54] H. Cao, T. Huang, M. Dai, X. Kong, H. Liu, Z. Zheng, G. Sun, G. Sun, D. Rong, Z. Jin, W. Tang, Y. Xia, Tumor microenvironment and its implications for antitumor immunity in cholangiocarcinoma: future perspectives for novel therapies, Int. J. Biol. Sci. 18 (14) (2022) 5369–5390, https://doi.org/10.7150/ijbs.73949.
[55] M.I. González, D.T. Vannan, B. Eksteen, I. Flores-Sotelo, J.L. Reyes, Mast cells in immune-mediated cholangitis and cholangiocarcinoma, Cells 11 (3) (2022), https://doi.org/10.3390/cells11030375.
[56] M. Zhang, C. Liu, Y. Li, H. Li, W. Zhang, J. Liu, L. Wang, C. Sun, Galectin-9 in cancer therapy: from immune checkpoint ligand to promising therapeutic target, Front. Cell Dev. Biol. 11 (2024) 1332205, https://doi.org/10.3389/fcell.2023.1332205.
[57] Y. Lv, X. Ma, Y. Ma, Y. Du, J. Feng, A new emerging target in cancer immunotherapy: Galectin-9 (LGALS9), Genes Dis 10 (6) (2023) 2366–2382, https://doi.org/10.1016/j.gendis.2022.05.020.
[58] J. Lv, Z. Jiang, J. Yuan, M. Zhuang, X. Guan, H. Liu, Y. Yin, Y. Ma, Z. Liu, H. Wang, X. Wang, Pan-cancer analysis identifies PD-L2 as a tumor promotor in the tumor microenvironment, Front. Immunol. 14 (2023) 1093716, https://doi.org/10.3389/fimmu.2023.1093716.
[59] T. Tanegashima, Y. Togashi, K. Azuma, A. Kawahara, K. Ideguchi, D. Sugiyama, F. Kinoshita, J. Akiba, E. Kashiwagi, A. Takeuchi, T. Irie, K. Tatsugami, T. Hoshino, M. Eto, H. Nishikawa, Immune suppression by PD-L2 against spontaneous and treatment-related antitumor immunity, Clin. Cancer Res. 25 (15) (2019) 4808–4819, https://doi.org/10.1158/1078-0432.Ccr-18-3991.
[60] O. Abdel-Rahman, Z. Elsayed, H. Elhalawani, Gemcitabine-based chemotherapy for advanced biliary tract carcinomas, Cochrane Database Syst. Rev. 4 (4) (2018), https://doi.org/10.1002/14651858.CD011746.pub2. Cd011746.